ISSN 2411-3336; e-ISSN 2541-9404

JOURNAL OF MINING INSTITUTE

Zapiski Gornogo instituta

Journal homepage: pmi.spmi.ru

Research article
UDC 669.712.054:553.411

# Mullite production: phase transformations of kaolinite, thermodynamics of the process

**Olga B. KOTOVA**[1], **Vladimir A. USTYUGOV**[1, 2] ✉, **Shiyong SUN**[3], **Alexey V. PONARYADOV**[1]

[1] *Institute of Geology Komi Science Center of Ural Branch of RAS, Syktyvkar, Russia*

[2] *Pitirim Sorokin Syktyvkar State University, Syktyvkar, Russia*

[3] *School of Environment and Resource, Southwest University of Science and Technology, People's Republic of China*

***How to cite this article***: Kotova O.B., Ustyugov V.A., Shiyong Sun, Ponaryadov A.V. Mullite production: phase transformations of kaolinite, thermodynamics of the process. Journal of Mining Institute. 2022. Vol. 254, p. 129-135. DOI: 10.31897/PMI.2022.43

***Abstract.*** The growing demand for mullite raw materials, which meet industrial requirements originates the search for new and alternative sources, as well as efficient technologies for obtaining the target products (nanocomposites). The article suggests a method for obtaining mullite from kaolinite experimentally (Vezhayu-Vorykvinsky deposit, Russia). Structural kaolinite transformations (Al-Si-O-Me system), mineral phases transformations, and thermodynamics of the process have been studied. Based on the estimation of the thermodynamics of the reactions, the preferable reaction of mullite formation was determined. The article shows, that formation of the target product, mullite nanocomposite, has several intermediate phases (metakaolinite, pseudomullite). The transformations of the initial kaolinite structure include the removal of structural water and separation of the silica-oxygen tetrahedral and alumina-oxygen octahedral layers, the decomposition into free oxides, breaking of bonds between the silica-oxygen tetrahedrons and the partial increase in the coordination number of aluminium ions, the formation of mullite and cristobalite from free oxides. The proposed approach controls the ratio of $Al_2O_3$ and $SiO_2$ phases at certain stages, which will further improve the mechanical and other properties of the matrix of the obtained raw materials for the target prototypes of industrial products.

***Keywords:*** kaolinite; phase transformations; mullite; thermodynamics; aluminosilicate systems; nanocomposites

***Acknowledgments.*** This work was supported by the Russian Science Foundation (project N 21-47-00019) and the National Natural Science Foundation of China (NSFC) N 42061134018.

***Received: 26.03.2022*** ***Accepted: 25.05.2022*** ***Online: 13.07.2022*** ***Published: 13.07.2022***

**Introduction.** Kaolinite and other clay minerals are widely used in various industries (nuclear power industry – as a major component of engineering barrier systems in the disposal of radioactive waste; construction; the production of ceramics and refractories, etc.) due to their high sorption properties and low water permeability [1-3]. Natural kaolin is usually used as kaolinite raw materials, which significantly reduces the cost of production. The main disadvantage of natural raw materials is the presence of impurities which affect the technological processes [4, 5] and the quality of the target product [6-8]. Currently, within the framework of global trends and technological challenges, including the production of high-tech ceramics and nanocomposites, the search for new approaches to the purity and composition of raw materials [9-10] and modeling of physical and chemical properties of target prototypes for various industrial applications is fundamental [11-13].

One of the most interesting prototypes for the industry is mullite ($Al_8[(O,OH,F)|(Si,Al)O_4]_4$) (aluminosilicate) and the highest temperature compound, $Al_2O_3$ with $SiO_2$, which is formed by heating kaolinite and other aluminosilicates [14-16], acquiring various physicochemical and technical

properties such as low thermal expansion and thermal conductivity, high creep resistance, high-temperature strength, and good chemical stability [17-19]. The main difficulty associated with the production of mullite is the need for high temperatures, which vary by several hundred degrees, depending on the methods and approaches used. Therefore, the issue of finding new effective approaches to obtain mullite-containing raw materials (as well as composites based on them) from new and alternative sources to obtain a given substance at lower temperatures remains relevant.

According to the history of the problem, the transition from the metastable high-alumina phase to the thermodynamically stable 3:2 mullite phase is a continuous process involving a continuous solid solution between the two mullite forms. Experimental work revealed a first-order phase transition between two different mullites [20-22]. Thus, a detailed study of the phase transformation of kaolinite during heating taking into account the thermodynamics of the process can improve the mechanical and other properties of the resulting matrix. Moreover, existing TS (TS 1569-00396495489-05, TS 14-8-447-83) and industrial standards for high alumina mullite raw materials determine the necessity of controlling the ratio of phases $Al_2O_3$ and $SiO_2$, as this parameter is decisive for further utilization of the obtained raw materials.

Many works have been devoted to the study of aluminosilicate systems since these systems are the basis of most technological processes for the production of "smart" materials (nanocomposites and nanoreactors) [23-25]. To study the reactions in Al-Si-O-Me aluminosilicate systems, mathematical modeling of processes [26-28] and thermodynamic analysis [19, 20, 29] are increasingly used to model the physical and chemical properties of mullite nanocomposite in various applications.

The purpose of this work is to obtain mullite experimentally from the Vezhayu-Vorykvinsky kaolinite deposit (corresponding to the industrial requirements and specifications) taking into account the thermodynamics of the aluminosilicate system. For this purpose, structural transformations of kaolinite (Al-Si-O-Me system), transformation of mineral phases, their physical and chemical properties depending on process thermodynamics were studied.

**Materials and research methods.** Kaolinite samples (Vezhayu-Vorykvinsky deposit, Knyazhpogostsky district, Komi Republic, 64°18′40.3″N, 51°08′31.5″E) were milled to a fraction of –0.1 mm (laboratory disc grinder LDI-65). Thermal treatment of samples in the temperature range 570-1470 K was carried out in the atmosphere of Carbolite Gero TF1 16/60/300 tube furnace, heating rate 10 K/min, holding time 2 h. The morphology of kaolinite samples (aluminosilicate systems $Al_2O_3$-$SiO_2$) was studied by scanning electron microscopy (TESCAN Vega 3). The phase composition of the samples was determined by diffractograms of unoriented samples. The images were taken on a Shimadzu XRD-6000 X-ray diffractometer, CuKα radiation, Ni-filter, 30 kV, 20 mA, scanning range 2-65° 2θ. The phase content was estimated by the Rietveld method (Profex software). The chemical composition was determined by X-ray fluorescence method (Shimadzu XRF-1800). IR spectra were obtained on a Fourier spectrometer InfraLUM FT-02 in the range of 400-4000 $cm^{-1}$ (KBr 1000:1.7 mg tablets). Thermogravimetric analysis was performed with a Mettler Toledo TGA/DSC 3+ (temperature range 300-1270 K, heating rate 10 K/min).

**Results and discussion.** *Study of material composition of initial kaolinite raw materials.* Complex analysis of chemical composition and $Al_2O_3/SiO_2$ ratio in kaolinite samples before experiments, mass%: $SiO_2$ 51.41; $Al_2O_3$ 43.79; $TiO_2$ 1.83; $Fe_2O_3$ 1.53; $K_2O$ 0.43; CaO 0.38; MgO 0.33. The ratio $Al_2O_3/SiO_2$ is 0.852, which is very close to the theoretical value of 0.85 for kaolinite.

X-ray phase analysis (XRD) showed that the original sample is kaolinite (~98 %) with minor impurities of diaspore and rutile (Fig.1). Interplanar distance of raw kaolinite diffractograms (Fig.2) is somewhat more than ideal and is 7.2 Å, and the reflex intensity is reduced, which suggests the existence of some amount of interlayer water between the silicate layers.

*Experimental studies.* During thermal treatment of kaolinite in the temperature range up to 720 K, its structure practically does not change (Fig.1).

DOI: 10.31897/PMI.2022.43

*Journal of Mining Institute.* 2022. Vol. 254. P. 129-135


At 770-820 K, an endothermic effect can be observed (Fig.2), which, according to IR-spectroscopy (Fig.3) is associated with the removal of hydroxyl groups, and at the end of the process the octahedral alumino-oxygen layer is almost completely replaced with tetrahedral alumino-oxygen layer of the intermediate X-ray amorphous phase (metakaolinite) which is probably connected between the layers via oxygen ions common to both the alumino and silico-oxygen layers (Si-O-Al bond) [9, 10]. On the diffractograms this disordered phase is characterized by diffuse reflexes (*d/n* ~ 4.4; 2.5; 1.7 Å), the basal peaks of kaolinite {001}, and periodicity along *c-axis* completely disappear. The peaks {−110} and {020} (2θ = 20-25°) – parameters of *a* and *b* axes – gradually become smooth and completely disappear at 1270 K. From 1340 K, another intermediate unidentifiable phase with diffuse reflexes (*d/n* ~ 4.0-3.9; 2.0-1.9 Å) appears. As the temperature increases further, the reflexes of these phases become more distinct and their interplanar distances change (*d/n* ~ 4.2; 2.5; 2.0 Å and pseudomullite with *d/n* ~ 4.0-3.9; 2.4; 1.9 Å respectively).

On the DSC curve (Fig.2) exothermic effect in the range of 1220-1270 K can be explained, probably, by the final destruction of kaolinite lattice, possible metakaolinite decomposition into free oxides, breaking of bonds between silica tetrahedrons and partial increase of coordination number of aluminium ions.

The mullite formation is fixed at 1470 K and characteristic diffraction peaks appear in the diffractogram. The crystal structure of mullite consists of paired chains $Si_2O_5$, in which the silicon ion is partially isomorphically replaced by an aluminium ion, which has both a six [$AlO_6$] and a four [$AlO_4$] coordination number. At the same temperature (1470 K) the appearance of the cristobalite phase is recorded, which formation is due to an excess of unbound silica (in mullite the Al/Si ratio is 3, whereas in the original kaolinite Al/Si = 2).

*IR spectroscopy.* IR spectra of the raw kaolinite and the annealed samples are shown in Fig.3. The characteristic absorption peak at 1101 $cm^{-1}$ was attributed to the valence vibrations of Si-O-Si of annealed kaolinite, the peak at 916 $cm^{-1}$ was attributed to the valence vibrations of Al-O in quaternary [AlO4] coordination, and the 575 $cm^{-1}$

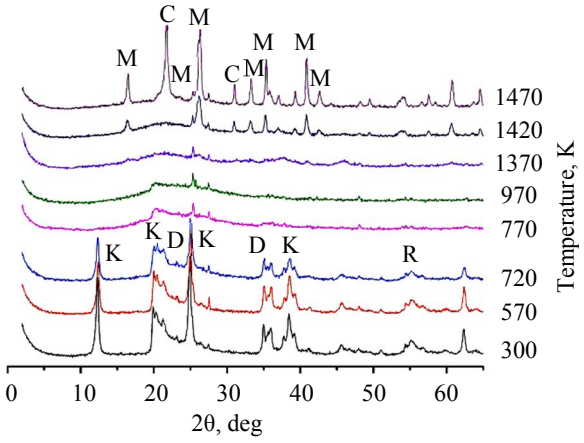


Fig.1. Diffractogram of raw kaolinite samples and annealed at different temperatures
K – kaolinite; D – diaspore; R – rutile; M – mullite; C – cristobalite

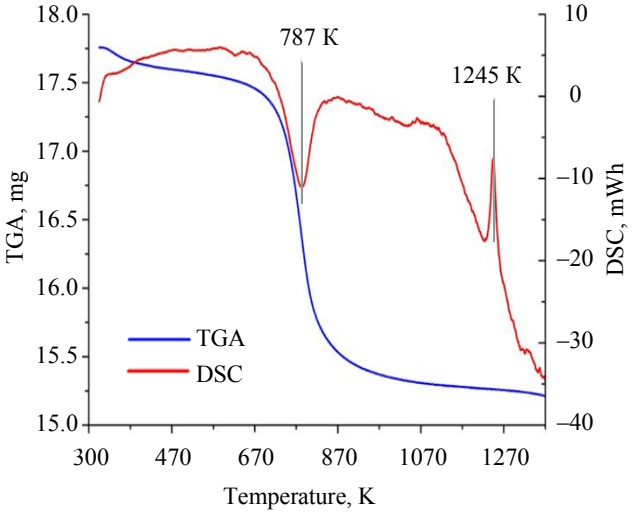


Fig.2. TGA and DSC curves of kaolinite samples

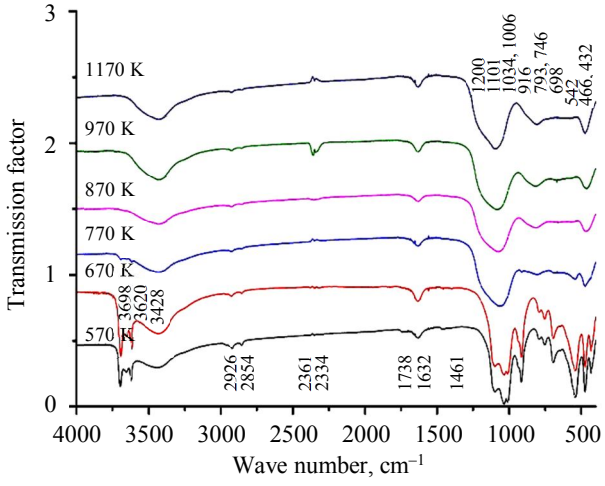


Fig.3. IR spectra of kaolinite samples treated at different temperatures

*Journal of Mining Institute.* 2022. Vol. 254. P. 129-135 DOI: 10.31897/PMI.2022.43


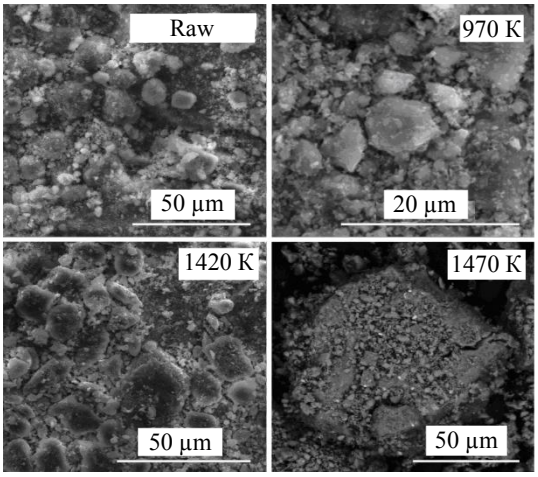


Fig.4. SEM images of raw kaolinite and annealed at different temperatures

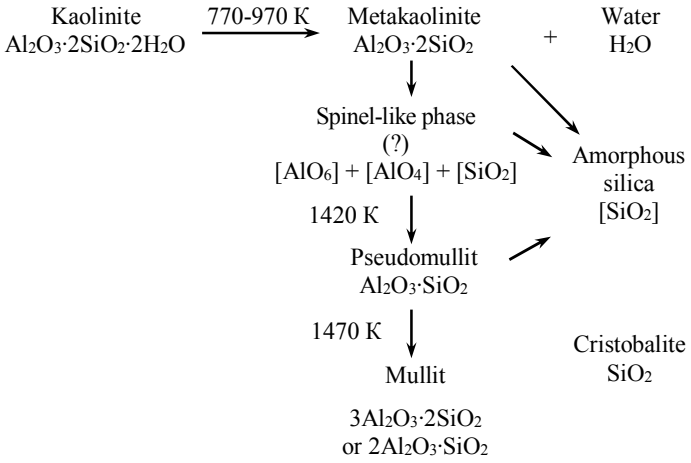


Fig.5. Chemical reactions of solid-phase transformation of kaolinite into mullite

peak is to the strain oscillations of Al-O in six-coordination [$AlO_6$] [30]. The 793 $cm^{-1}$ peak forming above 770 K was attributed to the Si-O bond in cristobalite and the characteristic 466 $cm^{-1}$ absorption peak to strain vibrations of Si-O. The peaks 746 $cm^{-1}$ and 542 $cm^{-1}$ are related to spinel-like phase formation [31]. The weakly pronounced peak at 1200 $cm^{-1}$, whose intensity decreases with increasing curing temperature, is related to amorphous silica (metakaolinite). The infrared spectra of kaolinite after temperature treatment are in agreement with the XRD results.

*Electron microscopy. The* sequence of these phase transformations can be traced on SEM: with increasing temperature there is a clear segregation of kaolinite grains, the formation of larger aggregates and clearly visible elements of its recrystallization (Fig.4). At temperature increase to 1420 K, short needle-like pseudomullite crystals appear on kaolinite surface. At 1470 K the surface of baked kaolinite particles is covered with needle crystals of pseudomullite and chaotically arranged grains of cristobalite. The given RFA, IR spectroscopy and SEM data are in a good agreement with the available literature data [21, 32].

*Kinetic analysis of mullite and cristobalite crystallization from kaolinite.* The data on mullite and cristobalite crystallization kinetics from kaolinite are given in paper [29]. The process of the solid-phase formation of mullite from kaolinite based on the X-ray phase analysis and infrared spectroscopy data is shown in Fig.5.

Based on experimental data, the thermodynamic process of kaolinite conversion can be represented as the following theoretical reactions:

$$\underset{\text{Kaolinite}}{Al_2O_3 \cdot 2SiO_2 \cdot 2H_2O} \Rightarrow \underset{\text{Metakaolinite}}{Al_2O_3 \cdot 2SiO_2} + 2H_2O;$$

$$\underset{\text{Metakaolinite}}{2(Al_2O_3 \cdot 2SiO_2)} \Rightarrow \underset{\text{Spinel (?)}}{2Al_2O_3 \cdot 3SiO_2} + SiO_2;$$

$$\underset{\text{Spinel (?)}}{2Al_2O_3 \cdot 3SiO_2} \Rightarrow \underset{\text{Pseudomullite}}{2(Al_2O_3 \cdot SiO_2)} + SiO_2;$$

$$\underset{\text{Pseudomullite}}{3(Al_2O_3 \cdot SiO_2)} \Rightarrow \underset{\text{Mullite}}{3Al_2O_3 \cdot 2SiO_2} + \underset{\text{Cristobalite}}{SiO_2}; \quad (1)$$

$$\underset{\text{Pseudomullite}}{2(Al_2O_3 \cdot SiO_2)} \Rightarrow \underset{\text{Mullite}}{2Al_2O_3 \cdot SiO_2} + \underset{\text{Cristobalite}}{SiO_2}. \quad (2)$$

Total reaction:

$$3(Al_2O_3 \cdot 2SiO_2 \cdot 2H_2O) \Rightarrow 3Al_2O_3 \cdot 2SiO_2 + 4SiO_2 + 6H_2O; \quad (3)$$

$$2(Al_2O_3 \cdot 2SiO_2 \cdot 2H_2O) \Rightarrow 2Al_2O_3 \cdot SiO_2 + 3SiO_2 + 4H_2O. \quad (4)$$

Considering the instability of chemical mullite composition (from $3Al_2O_3 \cdot 2SiO_2$ to $2Al_2O_3 \cdot SiO_2$), we propose its formation from pseudomullite (1) and (2) reactions, which, respectively, are reflected in total reactions (3) and (4).

The reactions given are pure reactions. Reactions involving the starting samples contain various impurities of iron oxides, titanium, etc. Assuming that in the first approximation the impurities have no influence on the final products, we use these reactions to calculate the Gibbs energy (isobaric potential) at different temperatures. Which of the reactions will be more preferable in terms of energy is determined by the value of the Gibbs energy change during the reaction [33].

To calculate the change in Gibbs energy, the thermodynamic Gibbs-Helmholtz relation relating enthalpy $H$ to Gibbs energy $G$ is used [34]:

$$H = -T^2 \left( \frac{\partial (G/T)}{\partial T} \right)_P.$$

By integrating this ratio, we bring it to this form:

$$G(T) = G_1 - T \int_{T_1}^{T} \frac{H(T)}{T^2} dT, \quad (5)$$

where $G_1$ is the Gibbs energy at temperature $T_1$; usually $T_1$ is taken as temperature $T = 298$ K, then instead of the integration constant $G_1$, the $\Delta G^0_{298}$ can be written, and instead of $G$ and $H$ we can use the changes of these parameters: $\Delta G$ is the change in Gibbs energy during the reaction, $\Delta H$ is the change in the heat of substances formation.

Then formula (5) will take the form:

$$\Delta G(T) = \Delta G^0_{298} - T \int_{298}^{T} \frac{\Delta H(T)}{T^2} dT. \quad (6)$$

In order to calculate using formula (6), it is necessary to know the enthalpy-temperature dependence, which is determined using the following formula:

$$\Delta H(T) = \Delta H^0_{298} + \int_{298}^{T} C_p(T) dT,$$

where $C_p(T)$ is the dependence of heat capacity on temperature, calculated by the interpolation formula:

$$C_p(T) = a + bT + \frac{c}{T^2}.$$

The constants $a$, $b$, $c$, $\Delta H^0_{298}$, $\Delta G^0_{298}$ for the substances included in the reaction are taken from the reference tables (Karapetiants M.Kh. Chemical thermodynamics. Moscow: Librocom, 2019, p. 584). For each individual reaction the constants are calculated by the following formulas:

$$\Delta a = \sum_{\text{Products}} \nu_i a_i - \sum_{\text{Raw materials}} \nu_j a_j;$$

$$\Delta b = \sum_{\text{Products}} \nu_i b_i - \sum_{\text{Raw materials}} \nu_j b_j;$$

$$\Delta c = \sum_{\text{Products}} \nu_i c_i - \sum_{\text{Raw materials}} \nu_j c_j;$$

*Journal of Mining Institute.* 2022. Vol. 254. P. 129-135 DOI: 10.31897/PMI.2022.43


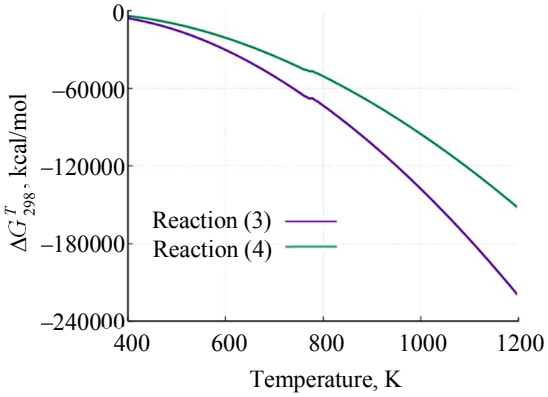


Fig.6. Gibbs energy variation as a function of temperature

$$\Delta G^0_{298} = \sum_{\text{Products}} \nu_i \left(\Delta G^0_{298}\right)_i - \sum_{\text{Raw materials}} \nu_j \left(\Delta G^0_{298}\right)_j;$$

$$\Delta H^0_{298} = \sum_{\text{Products}} \nu_i \left(\Delta H^0_{298}\right)_i - \sum_{\text{Raw materials}} \nu_j \left(\Delta H^0_{298}\right)_j,$$

where $\nu_i, \nu_j$ are stoichiometric coefficients.

The variation of the Gibbs energy as a function of temperature for reactions (3) and (4) is shown in Fig.6. According to thermodynamics, a system at constant temperature and pressure has the lowest Gibbs energy in the equilibrium state. The curve $\Delta G(T)$ for reaction (3) at any temperature goes lower, i.e., from the thermodynamic point of view, it is preferable.

**Conclusions.** For the first time, mullite has been obtained experimentally from kaolinite of Vezhayu-Vorykvinsky deposit taking into account the thermodynamics of the aluminosilicate system.

Experimental study of kaolinite phase transformation during heat treatment in the temperature range 670-1470 K was carried out. It is shown that the formation of the target product – mullite nanocomposite – proceeds in several phases: metacolinite, water, spinel phase, amorphous silica, pseudomullite.

The mullite phase is fixed at 1470 K with the appearance of cristobalite. The cristobalite formation is due to an excess of unbound silica (in mullite Al/Si = 3, whereas in the original kaolinite Al/Si = 2).

Transformations of the original kaolinite structure include removal of structural water with separation of the silica-oxygen tetrahedral and alumina-oxygen octahedral layers, decomposition to free oxides, breaking bonds between the silica-oxygen tetrahedrons, and the partial increase of the coordination number of aluminium ions, the formation of mullite and cristobalite from free oxides.

Based on the analysis of the chemical reaction thermodynamics, a less energy-consuming type of reaction to produce a mullite-containing nanocomposite has been determined. The proposed approach controls the ratio of phases $Al_2O_3$ and $SiO_2$ at certain stages, which will further improve the mechanical and the other properties of the matrix of the obtained raw materials for the target prototypes of industrial products.

## REFERENCES

1. Pusch R., Knutsson S., Al-Taie L., Mohammed M.H. Optimal ways of disposal of highly radioactive waste. *Natural Science*. 2012. Vol. 4. Special Issue, p. 906-918. DOI: 10.4236/NS.2012.431118

2. Sellin P., Leupin O.X. The use of clay as an engineered barrier in radioactive-waste management – a review. *Clay Minerals*. 2013. Vol. 61. Iss. 6, p. 477-498. DOI: 10.1346/CCMN.2013.0610601

3. Biswal B., Mishra D.K., Das S.N., Bhuyan S. Structural, micro-structural, optical and dielectric behavior of mullite ceramics. *Ceramics International*. 2021. Vol. 47. Iss. 22, p. 32252-32263. DOI: 10.1016/j.ceramint.2021.08.120

4. Evtushenko E.I., Sysa O.K., Lyashenko O.V., Novoselov A.G. Complex analysis of structural changes of hydrothermal-stabilized kaolins. *Vestnik Belgorodskogo gosudarstvennogo tekhnologicheskogo universiteta im. V.G.Shukhova*. 2012. N 3, p. 150-154 (in Russian).

5. Cui K., Zhang Y., Fu T. et al. Toughening Mechanism of Mullite Matrix Composites: A Review. *THE Coatings*. 2020. Vol. 10, p. 672-696. DOI: 10.3390/coatings10070672

6. Salakhov A.M., Salakhova R.A., Il'icheva O.M. et al. Influence of Material Structure on Ceramic Properties. *Vestnik Kazanskogo tekhnologicheskogo universiteta*. 2010. N 8, p. 343-349.

7. Al-Shantir O., Trník A., Csáki Š. Influence of firing temperature and compacting pressure on density and Young's modulus of electroporcelain. *AIP Conference Proceedings*. 2018. N 1988. DOI: 10.1063/1.5047595

8. De Aza A.H., Turrillas X., Rodriguez M.A. et al. Time-resolved powder neutron diffraction study of the phase transformation sequence of kaolinite to mullite. *Journal of the European Ceramic Society*. 2014. Vol. 34. Iss. 5, p. 1409-1421. DOI: 10.1016/j.jeurceramsoc.2013.10.034

9. Kotova O.B., Ignatiev G.V., Shushkov D.A. et al. Preparation and Properties of Ceramic Materials from Coal Fly Ash /Minerals: Structure, Properties, Methods of InvestigationSpringer.Proceedings in Earth and Environmental Sciences. Springer, Cham, 2019, p. 100-107. DOI: 10.1007/978-3-030-00925-0_16

10. Tong L.X., Li J.H., Liu F. Preparation of Mullite Nanocomposites Powders by the Hydrothermal Crystallization Method from Coal Gangue. *Key Engineering Materials*. 2012. Vol. 512-515, p. 49-53. DOI: 10.4028/www.scientific.net/KEM.512-515.49

11. Chandrasekhar S., Ramaswamy S. Influence of mineral impurities on the properties of kaolin and its thermally treated products. *Applied Clay Science*. 2002. Vol. 21, p. 133-142. DOI: 10.1016/S0169-1317(01)00083-7

12. Glinchuk M.D., Bykov I.P., Kornienko S.M. et al. Influence of Impurities on the Properties of Rare-Earth-Doped Barium-Titanate. *Journal of Materials Chemistry*. 2000. Vol. 10, p. 941-947. DOI: 10.1039/A909647G

13. Romero A.R., Elsayed H., Bernardo E. Highly porous mullite ceramics from engineered alkali activated suspensions. *Journal of the American Ceramic Society*. 2018. Vol. 101, p. 1036-1041. DOI: 10.1111/JACE.15327

14. Bai J. Fabrication and properties of porous mullite ceramics from calcined carbonaceous kaolin and α-Al2O3. *Ceramica International*. 2010. Vol. 36. Iss. 2, p. 673-678. DOI: 10.1016/J.CERAMINT.2009.10.006

15. Gustafsson S., Falk L.K., Pitchford J.E. et al. Development of Microstructure during Creep of Mullite and Mullite 5 vol% SiC Nanocomposite. *Journal of the European Ceramic Society*. 2009. Vol. 29. Iss. 4, p. 539-550. DOI: 10.1016/j.jeurceramsoc.2008.06.036

16. Lisuzzo L., Cavallaro G.P., Milioto S., Lazzara G. Halloysite nanotubes as nanoreactors for heterogeneous micellar catalysis. *Journal of Colloid and Interface Science*. 2021. N 608, p. 424-434. DOI: 10.1016/j.jcis.2021.09.146

17. Siteva O.S., Medvedeva N.A., Seredin V.V.et al. Influence of pressure on kaolinite structure in fire-clays of the Nizhne-Uvelskoedeposit by IR spectroscopy. *Bulletin of the Tomsk Polytechnic University. Geo Assets Engineering*. 2020. Vol. 331. N 6, p. 208-217 (in Russian). DOI: 10.18799/24131830/2020/6/2690

18. Botero C.A., Jimenez-Piqué E., Martín R. et al. Nanoindentation and Nanoscratch Properties of Mullite-Based Environmental Barrier Coatings: Influence of Chemical Composition-Al/Si Ratio. *Surface and Coatings Technology*. 2014. Vol. 239, p. 49-57. DOI: 10.1016/j.surfcoat.2013.11.016

19. Zhou H.M., Qiao X.C., Yu J.G. Influences of quartz and muscovite on the formation of mullite from kaolinite. *Applied Clay Science*. 2013. Vol. 80-81, p. 176-181. DOI: 10.1016/J.CLAY.2013.04.004

20. Jalilov A., Eshburiev T. Thermodynamic analysis of mullite formation from kaolinite. *Universum: Chemistry and Biology*. 2021. N 5 (83), p. 51-54 (in Russian).

21. Lamberov A.A., Sitnikova E.Yu., Abdulganeeva A.Sh. Influence of structure and composition of kaolinite clay on conditions of kaolinite-meta kaolinite transition. *Vestnik Kazanskogo tekhnologicheskogo universiteta*. 2011. N 7, p. 17-23 (in Russian).

22. Schmücker M., Schneider H., MacKenzie K.J.D. et al. $AlO_4/SiO_4$ distribution in tetrahedral double chains of mullite. *Journal of the American Ceramic Society*. 2005. Vol. 88. Iss. 10, p. 2935-2937. DOI: 10.1111/J.1551-2916.2005.00500.X

23. Abdrakhimov V.Z., Kolpakov A.V., Denisov D.Yu. Crystallization of mullite in the synthesis of ceramic materials from waste products. *Kontsept*. 2013. Vol. 3, p. 2716-2720 (in Russian).

24. Bartsch M., Saruhan B., Schmücker M., Schneider H. Novel Low-Temperature Processing Route of Dense Mullite Ceramics by Reaction Sintering of Amorphous $SiO_2$-Coated γ-$Al_2O_3$ Particle Nanocomposites. *Journal of the American Ceramic Society*. 2004. Vol. 82. N 6, p. 1388-1392. DOI: 10.1111/J.1151-2916.1999.TB01928.X

25. Sarkar R., Mallick M. Formation and densification of mullite through solid-oxide reaction technique using commercial-grade raw materials. *Bulletin of Materials Science*. 2018. Vol. 41, p. 1-8. DOI: 10.1007/s12034-017-1533-7

26. Dubovikov O.A., Nikolaeva N.V. Mathematical description of kaolinite decomposition process by alkaline solutions. *Journal of Mining Institute*. 2011. Vol. 192, p. 73-76 (in Russian).

27. Sperinck S., Raiteri P., Marks N., Wright K. Dehydroxylation of Kaolinite to Metakaolin – A Molecular Dynamics Study. *Journal of Materials Chemistry*. 2011. Vol. 21. Iss. 7, p. 2118-2125. DOI: 10.1039/C0JM01748E

28. Zhou Y., Liu Q., Xu P. et al. Molecular Structure and Decomposition Kinetics of Kaolinite/Alkylamine Intercalation Compounds. *Frontiers in Chemistry*. 2018. Vol. 6. N 310. DOI: 10.3389/fchem.2018.00310

29. Ondro T., Al-Shantir O., Csáki S. et al. Kinetic analysis of sinter-crystallization of mullite and cristobalite from kaolinite. *Thermochimica Acta*. 2019. Vol. 678. N 1783121. DOI: 10.1016/J.TCA.2019.178312

30. Dyatlova E.M., Bobkova N.M., Sergievich O.A. Infrared study of kaolin raw materials of belarusian deposits. *Problemy nedropolzovaniya*. 2019. N 2 (21), p. 143-149 (in Russian). DOI: 10.25635/2313-1586.2019.02.143

31. Weiquan Yuan, Jingzhong Kuang, Zheyu Huang, Mingming Yu. Effect of aluminum source on the kinetics and mechanism of mullite preparation from kaolinite. *Chemical Physics Letters*. 2022. Vol. 787. № 139242. DOI: 10.1016/j.cplett.2021.139242

32. Lee S., Kim Y., Moon H.-S. Phase Transformation Sequence from Kaolinite to Mullite Investigated by an Energy-Filtering Transmission Electron Microscope. *Journal of the American Ceramic Society*. 2004. Vol. 82, p. 2841-2848. DOI: 10.1111/J.1151-2916.1999.TB02165.X

33. Gmehling J., Kleiber M., Kolbe B.D., Rarey J. Chemical Thermodynamics for Process Simulation. Wiley-VCH, 2019, p. 805.

34. Fegley B. Practical Chemical Thermodynamics for Geoscientists. Elsevier, 2013, p. 813. DOI: 10.1016/C2009-0-22615-8

***Authors*: Olga B. Kotova,** *Doctor of Geological and Mineralogical Sciences, Chief Researcher, https://orcid.org/0000-0001-8448-3385 (Institute of Geology Komi Science Center of Ural Branch of RAS, Syktyvkar, Russia)*, **Vladimir A. Ustyugov,** *Candidate of Physics and Mathematics*, *Senior Researcher, ustyugovva@gmail.com, https://orcid.org/0000-0002-2238-1858 (Pitirim Sorokin Syktyvkar State University, Syktyvkar, Russia, Institute of Geology Komi Science Center of Ural Branch of RAS, Syktyvkar, Russia),* **Shiyong Sun,** *Doctor of Natural Sciences, Professor, https://orcid.org/0000-0001-5448-2701 (School of Environment and Resource, Southwest University of Science and Technology, People's Republic of China),* **Alexey V. Ponaryadov,** *Junior Researcher, https://orcid.org/0000-0003-1166-2408 (Institute of Geology Komi Science Center of Ural Branch of RAS, Syktyvkar, Russia).*

*The authors declare no conflict of interests.*